

Ferromagnetic Resonance of Horse Spleen Ferritin: Core Blocking and Surface Ordering Temperatures

Eliane Wajnberg,¹ Léa J. El-Jaick, Marília P. Linhares,* and Darci M. S. Esquivel

Centro Brasileiro de Pesquisas Físicas, and *Universidade Estadual do Norte Fluminense, Rio de Janeiro, Brazil

Received April 9, 2001; revised August 7, 2001; published online October 5, 2001

In nature, ferritin, an iron-storage molecule, is found in species ranging from bacteria to man. In the past 50 years its chemical, physical, and magnetic properties have been studied, searching to relate function and structure. Horse spleen ferritin has been investigated by EPR at temperatures between 7 and 290 K. These spectra change from an isotropic line at 290 K to an anisotropic one at 19 K, with a behavior consistent with a system of particles that undergoes superparamagnetic relaxation. A blocking temperature of (116 ± 9) K is obtained. A new temperature-dependent signal is observed in the low field region at temperatures higher than 80 K. At 7 K no EPR signal appears, suggesting (14 ± 5) K as the Néel temperature of surface spins. Analysis of the temperature dependence of the distance between EPR lines extrema, under the view of two theoretical models, allowed the evaluation of magnetic parameters. These parameters are $2K/M = 2.7 \times 10^3$ Oe and $MV = 1.9 \times 10^{-17}$ emu or $K/M = 1.3 \times 10^3$ Oe and $MV = 2.0 \times 10^{-17}$ emu, where K is the anisotropy energy per unit volume, M is the sample magnetization, and V is the superparamagnetic core volume. The results are also discussed, and some structural models in the literature are considered. © 2001 Academic Press

Key Words: horse spleen ferritin; EPR; blocking temperature; ordering temperature; magnetic moment; anisotropy field.

INTRODUCTION

Ferritin is an iron-storage protein in animals as well as in bacteria. The bulk of the iron in ferritin is known to be distributed as hydrous ferric oxide crystallites of various size up to 8 nm in diameter surrounded by a shell of protein of molecular weight 450,000 kDa, capable of storing up to 4500 iron atoms. The iron deposition in ferritin is the fundamental process by which cells store Fe^{3+} in a nontoxic but available form (1). The protein is an interesting subject for researchers in a range of fields: in biology, in the chemical synthesis of organic–inorganic nanostructures, and in the physics of magnetism. The chemical and physical properties of the iron core in ferritin are therefore clearly of interest. Magnetic resonance imaging as a model for contrast reagents and in the studies of iron deposits in patients has recently grown in importance (2).

Spectroscopic techniques provide an important approach to the study of the ferritin iron centers. The iron centers in ferritin have been extensively studied with a wide range of techniques such as extended X-ray absorption fine structure (EXAFS) (3, 4), Mössbauer spectroscopy (5–7), and magnetic measurements (8). However, EPR (electron paramagnetic resonance) measurements on mammalian holoferritin have been rather limited (6, 9–12).

Previous work has shown that two broad features characterize EPR spectra of horse spleen ferritin fractions with different iron/protein ratios (9). It has been shown that increasing the iron content in ferritin, the low-field feature, with a maximum near $g = 6$, increases while the high-field component, at about $g = 2$, decreases. The broad low-field feature was attributed to larger iron crystallites (9, 12), suggesting a relation of these features to a superparamagnetic behavior. Similar spectral changes would then be expected with temperature changes and were indeed noted in the papers of Weir *et al.* (11), Delghton *et al.* (12), and Boas and Troup (6). Although the latter considered the superparamagnetic properties of the cores to explain the broadening of the $g = 2$ line as temperature is lowered, the resonance at $g = 4$ (low-field feature) has not been related to the same characteristic.

In this paper we report on the temperature dependence of EPR spectra of horse spleen ferritin in order to assign their features to a superparamagnetic resonance behavior, extending the temperature range of measurements previously reported (6, 9, 11). This paper focuses on the use of EPR spectroscopy with quantitative analysis greater than that of previous papers. Analysis of the temperature dependence of the spectra under the view of two theoretical models previously proposed (13, 14) allowed the evaluation of magnetic parameters. Relevant temperatures of this antiferromagnetic nanoparticle system are also obtained. These results are discussed, and the recently proposed structural model differentiating between core and surface spins (15) is also considered.

MATERIAL AND METHODS

Horse spleen ferritin from Sigma was used with no further purification. A hundred microliters was transferred to sealed

¹ To whom correspondence should be addressed. E-mail: elianew@cbpf.br.

EPR tubes followed by nitrogen flux for a few minutes (samples A and B present different contributions of oxygen to the spectra as will be explained later). Another sample was nitrogen fluxed (sample C) until reduced to a wet paste. Annealing of horse spleen ferritin was performed for three consecutive periods of 20 min each, one at 350°C and two at 450°C.

EPR was performed with an X-band spectrometer (Bruker ESP300E) with 20 mW microwave power and 2 Oe field modulation over a temperature range from 7 to 290 K. A helium flux cryostat (Air Products) was used to control the temperature. Temperatures were measured with an Au-Fe x Chromel thermocouple just below the sample. The room temperature (RT) measurement was performed using a hematocrit capillar tube. Annealed sample spectra were obtained at RT. Field shifts due to different frequencies were corrected by means of the software WINSPEC that has been previously developed for manipulation of a set of EPR data of different spectrometers and formats. Curves were fitted using a Monte Carlo-like method (16) or Origin (Microcal) software.

RESULTS AND DISCUSSION

At temperatures lower than 80 K the spectra of sample A present contributions of residual oxygen in the atmosphere of the sample tube that render their analysis difficult. In this temperature range the spectra of sample B, which present a residual oxygen contribution much higher than that of the core signal, were used to minimize this contribution, subtracting them from the spectra of sample A, as shown in Fig. 1a.

EPR spectra present two features similar to those reported previously for ferritin cores, one centered at about $g = 2$ and another with a maximum near $g = 6$ (6, 9–12) with similar qualitative temperature behavior. The differences in the relative intensities of these two features can be due to factors affecting distribution of ferric ions in the cores, such as the presence of oxygen (aerobic/anaerobic conditions), pH, phosphate content, and aging (i.e., loss of water and rearrangement of ions) of core particles, reported for different ferritin samples and under different conditions (7a, 17).

When oxygen is completely removed before measurement (sample C), the core signal disappears and only the $g = 2.066$ radical line and the $g = 4.3$ iron feature are observed (Fig. 1b). A $g = 2.066$ line is also present in the spectra of Fig. 1a. A similar line was observed for a radical formation when the ferritin core is developed from Fe^{2+} and O_2 in apoferritin. It was strongly suggested that the radical is a by-product of core formation (18).

The $g = 4.3$ line was assigned to the presence of non aggregated Fe^{3+} bound in a protein site of low symmetry in bacterioferritin spectra (19). It was suggested on the basis of EPR studies that additional monomeric loose iron is associated with the protein shell to solitary high-spin Fe^{3+} ions bound to apoferritin when Fe^{2+} is added followed by air oxidation (20).

At temperatures higher than 80 K the spectra also contain a narrow signal in the region of $g = 9$ not yet reported for horse

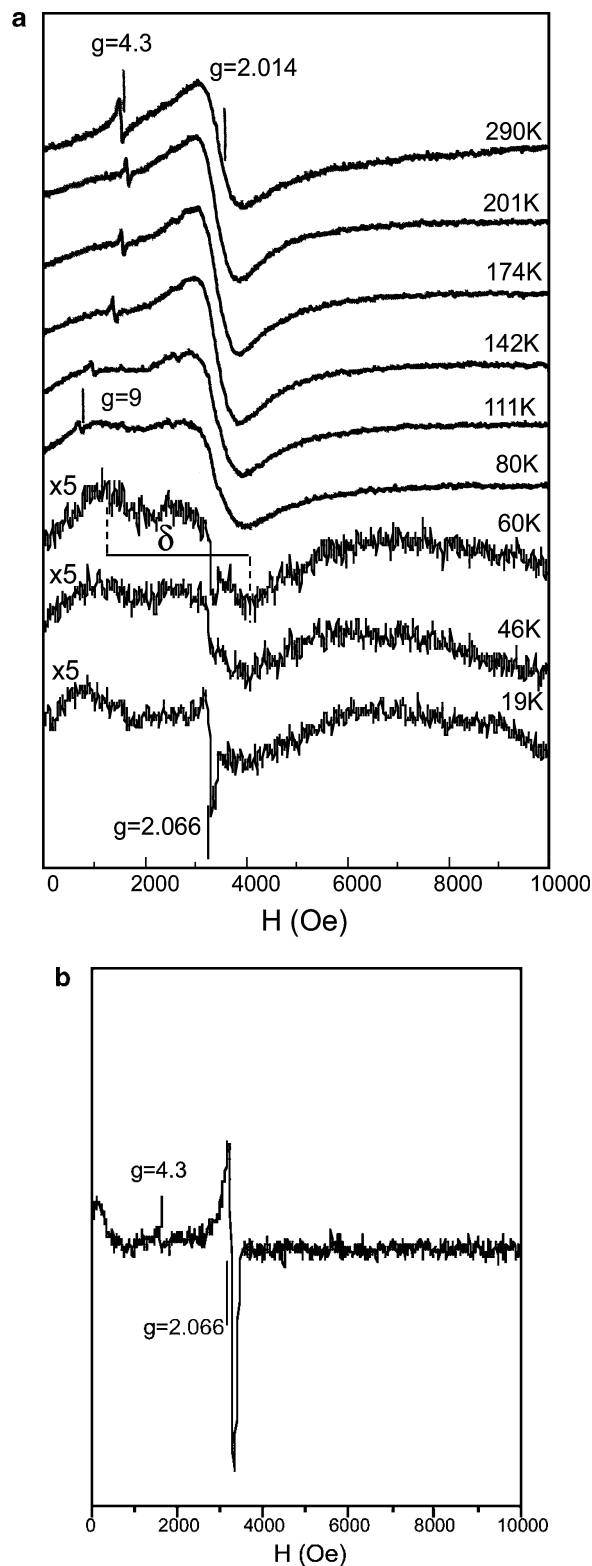


FIG. 1. (a) EPR spectra of horse spleen ferritin as a function of temperature (sample A). At temperatures lower than 80 K, the contribution of the residual oxygen was subtracted as described in the text; (b) EPR spectrum of horse spleen ferritin, at 7.5 K, where oxygen is completely removed before measurement (sample C).

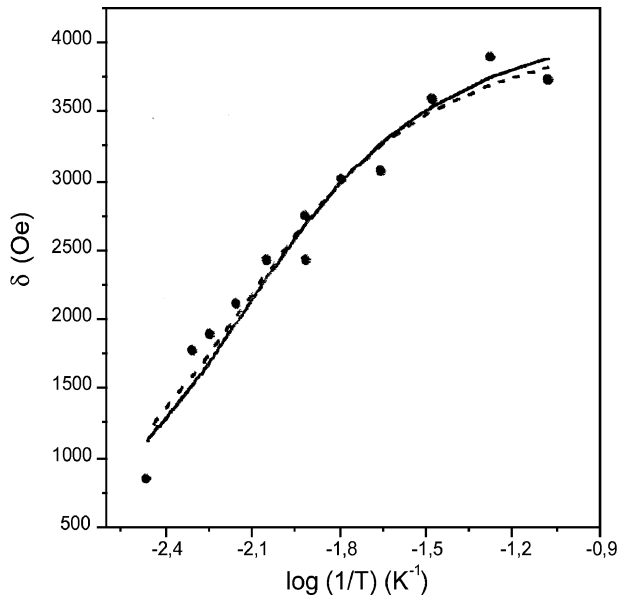


FIG. 2. Temperature dependence of the distance between EPR lines extrema, δ . The solid line is the best fit of the δ data according to Eq. [1], from model 1, with $H_{\text{bulk}} = 2K/M = 2.7 \times 10^3$ Oe and $MV = 1.9 \times 10^{-17}$ emu. The dashed line is the best fit according to Eq. [2] from model 2, with $K/M = 1.3 \times 10^3$ Oe and $MV = 2.0 \times 10^{-17}$ emu.

spleen ferritin, as far as we know, the intensity of which increases with temperature and its position moves toward the lower $g = 4$ region (see Fig. 1a).

At 290 K the core spectrum is characterized by a broad line centered at $g = 2.014$ that decreases in intensity and increases in linewidth as temperature is lowered. At low temperatures the spectra are anisotropic with a low-field feature previously observed (6, 9, 11, 12). This behavior is consistent with a superparamagnetic resonance theory (13, 14). Signal is no longer observed when the temperature is lowered to 9 K.

The temperature dependence of the distance between EPR line extrema, δ (measured as shown in Fig. 1a), was used to study the system properties of superparamagnetic particles. The results are plotted in Fig. 2. Two models (13, 14) were used to analyze this temperature dependence of EPR spectra by considering the magnetic anisotropy field to be larger than the single-crystal linewidth.

The superparamagnetic apparent anisotropy field, H_{SP} with an axial symmetry is given by (13)

$$H_{\text{SP}}/H_{\text{bulk}} = (1 - 3x^{-1} \coth x + 3x^{-2})/(\coth x - x^{-1}), \quad [1]$$

where $x = MVH/k_B T$ and V is the superparamagnetic particle volume. H_{bulk} is the bulk anisotropy field, expressed as $2K/M$, where M is the sample magnetization, K the anisotropy constant, and H is the external applied field. This expression supposes that the system consists of small noninteracting particles embedded in a diamagnetic matrix and all particles have

the same intrinsic moment, anisotropy constant, and volume. Although the last one is not satisfied for ferritin molecules, which certainly present a core volume distribution, calculations based on this model can provide some limiting or average values and strengthen the hypothesis of superparamagnetic behavior. The parameter values could also be achieved by taking into consideration this volume distribution of the ferritin cores in the fittings; nevertheless the quality improvement would not be significant considering the experimental error and temperature intervals.

The solid curve in Fig. 2 is calculated from the fitting of $\delta = 3H_{\text{SP}}/2$ as shown by Griscom (21) for the axial symmetry case with H_{SP} given by Eq. [1]. The combination of these two equations will be called model 1. MV and H_{bulk} are the fitting parameters with best values $H_{\text{bulk}} = 2K/M = 2.7 \times 10^3$ Oe and $MV = 1.9 \times 10^{-17}$ emu, resulting in an anisotropy energy $KV = 2.5 \times 10^{-14}$ erg. Although the external field H varied, its effect on the δ expression was negligible, then it was taken as 3000 Oe to calculate x in Eq. [1].

Model 2 (14) proposes that, for a randomly oriented uniaxial system of ferromagnetic particles, the distance, δ , is given by $\delta = \delta_s + \delta_u$, where δ_s is the superparamagnetic broadening and δ_u is the inhomogeneous broadening. $\delta_{s,u}$ are written as a function of the Langevin parameter $\xi_0 = MV\omega/\gamma k_B T$, where ω is the Larmor frequency (here 5.9×10^{10} rad/s) and γ is the gyromagnetic ratio (2×10^7 erg/Oe). Given the dimensionless precession damping $\alpha = 0.01$ (as suggested in Ref. (14)), the dimensionless anisotropy parameter $\varepsilon = K\gamma/M\omega$, and the Langevin functions $L_{1,2}$, we have

$$\delta_s = \omega\alpha(\xi_0 - L_1)/(3^{1/2}\gamma\xi_0 L_1) \quad \text{and} \quad \delta_u = 3\omega\varepsilon L_2/\gamma L_1. \quad [2]$$

Taking K/M and MV as the fitting parameters in Eq. [2], we obtained the dashed curve in Fig. 2 with $K/M = 1.3 \times 10^3$ Oe and $MV = 2.0 \times 10^{-17}$ emu, yielding $KV = 2.6 \times 10^{-14}$ erg. These values are similar to those obtained using the previous model.

Superparamagnetic particles undergo thermally induced rotations of the magnetization with a relaxation time τ . The EPR spectral shape depends on the magnitude of τ relative to the observation time of the measurement and, as τ is a function of temperature, there will be in theory a certain temperature, namely the blocking temperature, T_b , at which the spectrum shape changes. However, in practice, a sample of ferritin normally contains a range of core sizes and this leads to a T_b distribution and the characteristic coexistence of components in the spectra. Considering, for simplicity, that the EPR spectra consist of two components—one isotropic due to unblocked small particles (temperatures higher than T_b) and another anisotropic due to a blocked magnetic phase (temperatures lower than T_b)—the relative fractions of these components can be obtained as a function of temperature. A computer fitting of the spectra could give this ratio but the following approach is intrinsically simpler and just as reliable. The intensity of the spectrum at a given magnetic field is the sum of these weighted components, depending

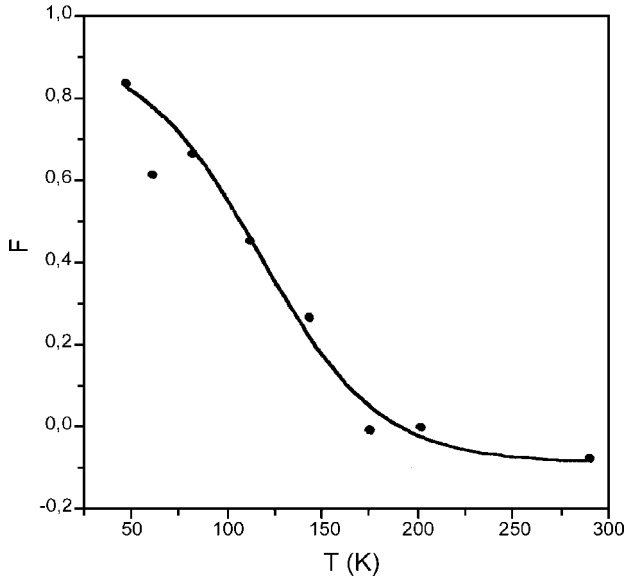


FIG. 3. Temperature dependence of the normalized fraction of ordered magnetic clusters obtained from Eq. [3] at the constant field of 1123 Oe ($g = 6.0$). The solid line is a guide to the eyes.

on their fractions. The normalized fraction of ordered magnetic clusters, F , is given in Fig. 3 as a function of temperature. The fraction F was obtained from the intensities ratio at the constant field of 1123 Oe ($g = 6.0$) as

$$F = (I - I_{\text{iso}})/(I_{\text{anis}} - I_{\text{iso}}), \quad [3]$$

where I_{iso} and I_{anis} are the intensities at the limiting isotropic (high-temperature) and anisotropic spectra (low-temperature) conditions, respectively. F decreases with increasing temperatures from above ~ 50 K.

In analogy to Mössbauer spectroscopy, an average blocking temperature, $\langle T_b \rangle$, is taken as the temperature at which the magnetic fraction is 0.5 ($F = 0.5$) (7, 24). From Fig. 3, $\langle T_b \rangle$ is (116 ± 9) K, obtained from fitting the data to a sigmoid function, the solid line, used as a guide to the eye.

The temperature dependence of the resonant magnetic field of the monomeric iron is shown in Fig. 4. We consider that this anomalous behavior is due to an internal field, H_{int} , so that $H_{\text{res}} = H_0 - H_{\text{int}}$, where H_0 is the resonant field of the isolated iron. H_{int} can be associated to the presence of the anisotropy field, H_{SP} . At high temperatures the magnetization of the core is substantially reduced, and the anisotropy field becomes negligible, so that $H_{\text{res}} = H_0$. Within this approximation, the limiting expression of Eq. [1] for H_{SP} , with $x \ll 1$ is $H_{\text{int}} = H_{\text{SP}} = 2KVH/5k_B T$. If we consider $H = H_{\text{res}}$,

$$(H_{\text{res}} - H_0)/H_{\text{res}} = 2KV/5k_B T. \quad [4]$$

The best fitting values $2KV/5k_B = (164 \pm 95)$ K and $H_0 = (2.7 \pm 0.8) \times 10^3$ Oe give the solid line in Fig. 4, resulting in an

average value $\langle KV \rangle$ of $(5.6 \pm 3.3) \times 10^{-14}$ erg, in agreement with that obtained from the linewidth analysis.

Previous EPR (6, 9, 11, 12) studies of horse spleen ferritin have considered the spectra as composed of two components at high and low fields. Our interpretation follows more closely model 1 (13, 21) and model 2 (14). In this paper we propose that the broad line, characterized by $g = 2.014$ at $T = 290$ K, in the core spectra (Fig. 1a) is resultant of a collection of superparamagnetic particles. Rotations of the magnetization vector can be thermally induced with a relaxation time, t_{sp} . For long t_{sp} , when compared to the measurement time, t (blocked particles), an anisotropic spectrum is obtained from a spread in the orientation of the magnetization. If t_{sp} is shorter than t (unblocked particles), the effective anisotropy decreases and a narrower isotropic line is observed. This is due to averaging over the observation time of the interactions, which gives rise to the broad spectrum. t_{sp} increases with the ratio between the anisotropy energy, KV , and the thermal energy, $k_B T$. Similarly, nucleation of small particles induced by annealing increases t_{sp} , yielding highly anisotropic spectra for heated ferritin, which are compared to the spectra of native ferritin at RT and 80 K in Fig. 5.

Because of the volume dependence of K it is more plausible to compare anisotropy energies KV (7a) than anisotropy constants K . The KV value of 2.6×10^{-14} erg obtained from models 1 and 2 mentioned above is compatible to the range of values found by Bell *et al.* (22) from 0.74×10^{-14} erg for a volume of 84×10^{-21} cm³ up to 2.6×10^{-14} erg for 182×10^{-21} cm³.

The blocking temperature depends on the experimental technique because each technique has a characteristic measurement time. Thus with two different techniques the corresponding values of T_{b1} and T_{b2} can be found. Considering the Néel–Arrhenius

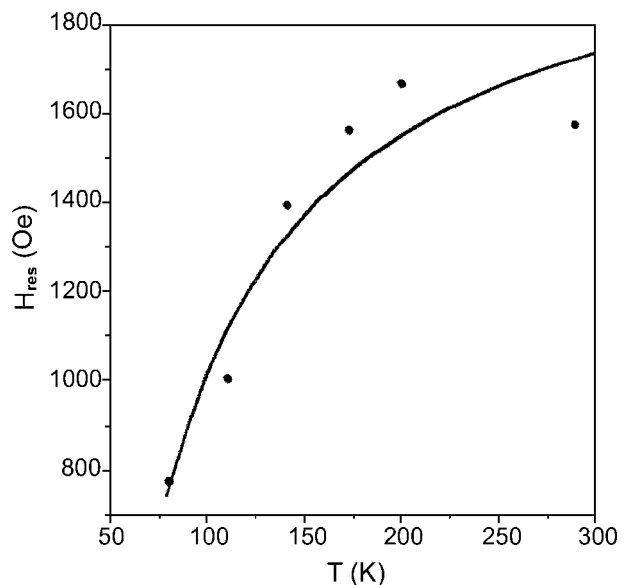


FIG. 4. Temperature dependence of the resonant magnetic field of the monomeric iron. The solid line is the best fit of Eq. [4] with $2KV/5k_B = (164 \pm 95)$ K and $H_0 = (2.7 \pm 0.8) \times 10^3$ Oe.

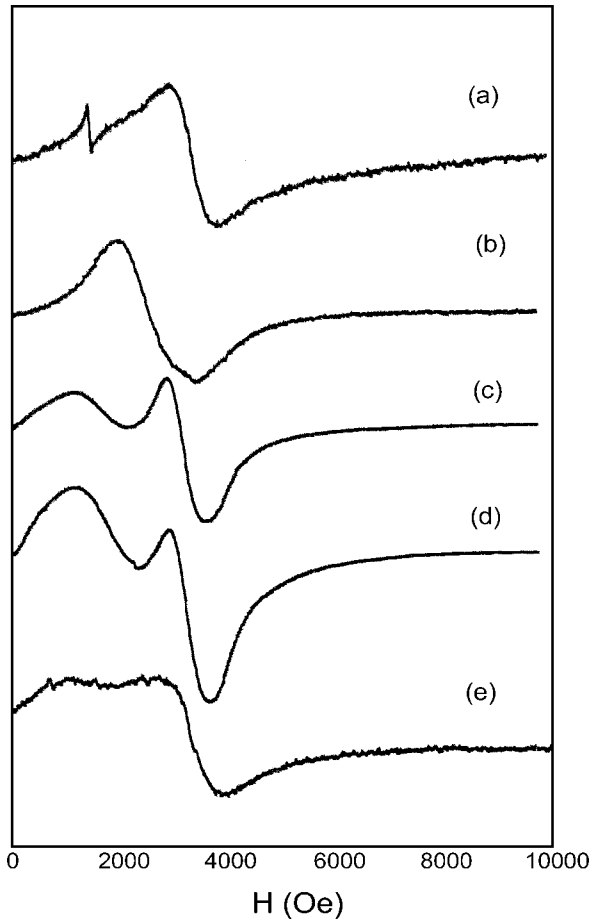


FIG. 5. (a) Native horse spleen ferritin spectrum (sample A) at RT; (b)–(d) RT spectra of the same sample A annealed for 20-min consecutive periods, each at 350, 450, and 450°C, respectively; (e) native horse spleen ferritin spectrum (sample A) at 80 K.

expression $t_{sp}^{-1} = f_0 \exp(-\Delta E_a/k_B T_b)$, the preexponential factor, f_0 , when ΔE_a (median anisotropy energy) is the same for both techniques, is given by (23)

$$f_0 = [t_1^\beta / t_2]^{1/1-\beta}, \quad [5]$$

where $\beta = T_{b1}/T_{b2}$ is the ratio of the average blocking temperatures determined by experiments with measurement times t_1 and t_2 . f_0 was determined as $(5.4 \pm 2.4) \times 10^{11}$ Hz for horse spleen ferritin using a combination of magnetic ($T_b = 9 \pm 2$ K, $t = 100$ s) and Mössbauer ($T_b = (36 \pm 1)$ K, $t \geq 5 \times 10^{-9}$ s) experiments (23). With these values Eq. [5] gives an estimate of $T_b \geq 72$ K for an EPR experiment with $t = 1.05 \times 10^{-10}$ s. Considering other reported T_b values from magnetic measurements, as 12 ± 1 K (24, 25), $T_b = 98 \pm 11$ K is expected for EPR measurements. We obtained a blocking temperature $T_b = (116 \pm 9)$ K, from the fitting in Fig. 3, which is in good agreement with the estimates above for EPR.

Iron cores of ferritin are proposed to consist of antiferromagnetically ordered Fe^{3+} ions (24), occurring in a transition to a state of ordered spins, with zero resultant magnetic moment, below the ordering temperature, T_{ord} , called the Néel point. T_{ord} derived from Mössbauer experiments has T_b as an upper limit, but 240 K is widely accepted as T_{ord} for natural horse spleen ferritin (7b, 8a). Below this temperature the incomplete cancellation of sublattices results in a net magnetic moment, giving rise to the EPR signal. The EPR signal of horse spleen ferritin core disappears for temperatures lower than 14 ± 5 K, indicating zero magnet moment and suggesting this temperature as the T_{ord} . Although this effect was not observed before for a freeze-dried sample with low iron content (10), no resonance were observed at 4.2 K for a ferritin wet paste (6). This temperature is much lower than the ordering temperature estimated by Mössbauer spectroscopy, but it can be understood under the view of the new structure proposed for the ferritin core. Combined nuclear magnetic relaxometry and magnetometry measurements suggest an interior of the core with a Néel temperature higher than 37°C and an external core region, where the Néel temperature is no higher than 30 K (15). The low-temperature transition observed by EPR is in good agreement with the antiferromagnetic transition of the surface ions in ferritin cores.

The isolated iron line ($g = 4.3$) has only been observed by EPR in low-iron-content horse protein during core formation (20) and in natural bacterioferritin (19); nevertheless Mössbauer studies (7a) suggested that the last-in ferric ions form smaller clusters or domains within the horse ferritin core. Our results indicate the presence of monomeric iron in natural horse spleen ferritin, which should be close enough to the core to be subjected to its magnetic anisotropy field. At the lowest temperatures the resonance field is 730 Oe ($g = 9$) instead of 1530 Oe as expected ($g = 4.3$), then the core is contributing with a magnetic field of ~ 800 Oe at the iron site. As the anisotropy magnetic field H_A is ~ 2700 Oe at the core surface with a mean radius of 27 Å (24), we can estimate roughly the distance of the monomeric iron from the center of the core as ~ 40 Å, taking an $1/r^3$ dependence for the magnetic field decay. This estimate favors the cavity surface carboxyl suggested by Bauminger *et al.* (5) as a conceivable site for binding isolated Fe^{3+} .

It was shown that the magnetic parameters of horse spleen ferritin can be determined by EPR based on a superparamagnetic model but the data presented do not unequivocally support any one of the two models used in this paper. Corrections taking into consideration the volume distribution of the ferritin cores can improve the results. The parameters obtained are in good agreement with those determined by other spectroscopic techniques. Considering a different interpretation for magnetic experiments in ferritin, evidence for paramagnetic Curie–Weiss iron ions at the core surface, where the local Néel temperature is very low, has been provided. The T_{ord} value, 14 ± 5 K, obtained in this paper supports this recently proposed core structure (15). Nevertheless, further theoretical developments should be

stimulated, considering that the observed anomalies for ferritin are still not fully understood.

ACKNOWLEDGMENTS

The authors thank E. F. Pessoa for the development of Winspec, and G. Cantalluppi for preliminary fittings. D. M. S. Esquivel and E. Wajnberg thank CNPq for financial support.

REFERENCES

1. P. M. Harrison, P. J. Artymiuk, G. C. Ford, D. M. Lawson, J. M. A. Smith, A. Treffy, and J. L. White, Ferritin: Function and structural design of an iron-storage protein, in "Biom mineralization, Chemical and Biochemical Perspectives" (S. Mann, J. Webb, and R. J. P. Williams, Eds.), pp. 257–294, VCH, Weinheim (1989).
2. T. G. St. Pierre, P. Chan, K. R. Bauchspiess, J. Webb, S. Betteridge, S. Walton, and D. P. E. Dickson, Synthesis, structure and magnetic properties of ferritin cores with varying composition and degrees of structural order: models for iron oxide deposits in iron-overload diseases, *Coord. Chem. Rev.* **151**, 125–143 (1996).
3. S. M. Heald, E. A. Stern, B. Bunker, E. M. Holt, and S. L. Holt, Structure of the iron-containing core in ferritin by the extended X-ray absorption fine structure technique, *J. Am. Chem. Soc.* **101**, 67–73 (1979).
4. J. S. Rohrer, Q. T. Islam, G. D. Watt, D. E. Sayers, and E. C. Theil, Iron environment in ferritin with large amounts of phosphate, from *Azotobacter vinelandii* and horse spleen, analyzed using extended X-ray absorption fine-structure (EXAFS), *Biochem.* **29**, 259–264 (1990).
5. E. R. Bauminger, P. M. Harrison, D. Hechel, I. Nowik, and A. Treffy, Mössbauer spectroscopic investigation of structure-function relations in ferritins, *Biochim. Biophys. Acta* **1118**, 48–58 (1991).
6. J. F. Boas and G. J. Troup, Electron spin resonance and Mössbauer effect studies of ferritin, *Biochim. Biophys. Acta* **229**, 68–74 (1971).
7. (a) R. B. Frankel, G. Papaefthymiou, and G. D. Watt, Variation of superparamagnetic properties with iron loading in mammalian ferritin, *Hyperfine Interact.* **66**, 71–82 (1991); (b) E. R. Bauminger and I. Nowik, Magnetism in plant and mammalian ferritin, *Hyperfine Interact.* **50**, 489–497 (1989).
8. (a) D. D. Awschalom, J. F. Smyth, G. Grinstein, D. P. DiVincenzo, and D. Loss, Macroscopic quantum tunneling in magnetic proteins, *Phys. Rev. Lett.* **68**, 3092–3095 (1992); (b) J. Tejada and X. X. Zhang, On magnetic relaxation in antiferromagnetic horse-spleen ferritin proteins, *J. Phys.: Condens. Matter* **6**, 263–266 (1994).
9. M. P. Weir, J. F. Gibson, and T. J. Peters, An electron paramagnetic resonance study of ferritin and haemosiderin, *Biochem. Soc. Trans.* **12**, 316–317 (1984).
10. S. Aime, B. Bergamasco, D. Biglino, G. Digilio, M. Fasano, E. Giamello, and L. Lopiano, EPR investigations of the iron domain in neuromelanin, *Biochim. Biophys. Acta* **1361**, 49–58 (1997).
11. M. P. Weir, T. J. Peters, and J. F. Gibson, Electron spin resonance studies of splenic ferritin and haemosiderin, *Biochim. Biophys. Acta* **828**, 298–305 (1985).
12. N. Delgton, A. Abu-Raqabah, I. J. Rowland, and M. C. R. Symons, Electron paramagnetic resonance studies of a range of ferritins and haemosiderins, *J. Chem. Soc., Faraday Trans.* **87**, 3193–3197 (1991).
13. R. S. de Biasi and A. A. R. Fernandes, Ferromagnetic resonance evidence for superparamagnetism in a partially crystallized metallic glass, *Phys. Rev. B* **42**, 527–529 (1990); R. S. de Biasi and T. C. Devezas, Anisotropy field of small magnetic particles as measured by resonance, *J. Appl. Phys.* **49**, 2466–2469 (1978).
14. Y. L. Raikher and V. I. Stepanov, The effect of thermal fluctuations on the FMR line shape in dispersed ferromagnets, *Sov. Phys. JETP* **75**, 764–771 (1992).
15. R. A. Brooks, J. Vymazal, R. B. Goldfarb, J. W. M. Bulte, and P. Aisen, Relaxometry and magnetometry of ferritin, *Magn. Reson. Med.* **40**, 227–235 (1998).
16. P. C. Taylor and P. J. Bray, Computer simulations of magnetic resonance spectra observed in polycrystalline and glassy samples, *J. Magn. Reson.* **2**, 305–331 (1970).
17. E. R. Bauminger, P. M. Harrison, I. Novik, and A. Treffy, Mössbauer spectroscopic study of the initial stages of iron core formation in horse spleen δ : Evidence for both isolated Fe(III) atoms and oxo-bridged Fe(III) dimers as early intermediates, *Biochemistry* **28**, 5486–5493 (1989).
18. J. K. Grady, Y. Chen, N. D. Chasteen, and D. C. Harris, Hydroxyl radical production during oxidative deposition of iron in ferritin, *J. Biol. Chem.* **264**, 20,224–20,229 (1989).
19. M. R. Cheesman, F. H. A. Kadir, J. Al-Basseet, F. Al-Massad, J. Farrar, C. Greenwood, A. J. Thomson, and G. R. Moore, E. P. R. and magnetic circular dichroism spectroscopic characterization of bacterioferritin from *Pseudomonas aeruginosa* and *Azobacter vinelandii*, *Biochem. J.* **286**, 361–367 (1992).
20. N. D. Chasteen, B. C. Antanaitis, and P. Aisen, Iron deposition in Apoferritin, *J. Biol. Chem.* **260**, 2926–2929 (1985).
21. D. L. Griscom, Ferromagnetic resonance spectra of lunar fines: Some indications of line shape analysis, *Geochim. Cosmochim. Acta* **38**, 1509–1519 (1974).
22. S. H. Bell, M. P. Weir, D. P. E. Dickson, J. F. Gibson, G. A. Sharp, and T. J. Peters, Mössbauer, spectroscopic studies of human haemosiderin and ferritin, *Biochim. Biophys. Acta* **787**, 227–236 (1984).
23. D. P. E. Dickson, N. M. K. Reid, C. Hunt, H. D. Williams, M. El-Hilo, and K. O'Grady, Determination of f_0 for fine magnetic particles, *J. Magn. Magn. Mater.* **125**, 345–350 (1993).
24. S. Gider, D. D. Awschalom, T. Douglas, S. Mann, and M. Chaparala, Classical and quantum magnetic phenomena in natural and artificial ferritin proteins, *Science* **268**, 77–80 (1995).
25. A. S. Makhlof, F. T. Parker, and A. E. Berkowitz, Magnetic hysteresis anomalies in ferritin, *Phys. Rev. B* **55**, 14,717–14,720 (1997).